Supplementary Materials for

Sulfate was a trace constituent of Archean seawater

Sean A. Crowe,* Guillaume Paris, Sergei Katsev, CarriAyne Jones, Sang-Tae Kim, Aubrey L. Zerkle, Sulung Nomosatryo, David A. Fowle, Jess F. Adkins, Alex L. Sessions, James Farquhar, Donald E. Canfield

*Corresponding author. E-mail: sacrowe1@gmail.com

Published 7 November 2014, *Science* **346**, 735 (2014)
DOI: 10.1126/science.1258966

This PDF file includes:

Other Supplementary Material for this manuscript includes the following:
(available at www.sciencemag.org/content/346/6210/735/suppl/DC1)

Materials and Methods

Measurements of $\delta^{34}S$ were made by Isotope Ratio Mass Spectrometry following sulfur conversion to either SF_6 or SO_2. Measurements of $\delta^{34}S$ values at low sulfate concentrations were made by MC-ICP-MS (*20*). The isotope fractionation factor (α) was calculated as $\ln(R/R_0)=(1/\alpha-1) \times \ln(S/S_0)$, where R is $^{34}S/^{32}S$, and S is sulfate concentration. The subscript '0' indicates the sulfate concentration and isotopic composition of the surface water. The fractionation factor (α) is related to ε by $\varepsilon=(\alpha-1) \times 1000$ and $\varepsilon \approx (\delta^{34}S\text{-}SO_4 - \delta^{34}S\text{-}HS)$. Residence times were calculated by multiplying the sulfate concentration in a compartment by the volume of that compartment and dividing by the sulfate removal flux, which at steady state is equal to the sulfate addition flux. We used published ranges for sulfate addition fluxes (*30*).

Supplementary Text

Lake Matano 1-dimensional reaction-transport model

To model S-isotope fractionation in an open system, we setup a 1-dimensional reaction-transport model in which the profiles of the individual S-isotopes were described independently. Similar models have been constructed in marine sediments (*22*). The model predicts sulfate distributions under steady-state conditions by describing changes in sulfate concentrations with depth as a function of rates of vertical transport and bacterial reduction of sulfate to sulfide as:

$$K_z \frac{d^2[SO_4^{2-}]}{dx^2} - R_{SR} = 0$$

where K_z is the eddy diffusion coefficient (0.1 m^2d^{-1} in the redoxcline of Lake Matano, (*33*)), x is the depth in the water column, and R_{SR} is the sulfate reduction rate.

Rates of sulfate reduction (R_{SR}) in the model were set with an explicitly specified depth distribution function to generate modeled sulfate profiles that fit the measured sulfate profiles. Sulfate reduction rates were thus set for a normal distribution:

$$R = R_0 \frac{1}{\sigma\sqrt{2\pi}} e^{\frac{1}{2}\left(\frac{x-\mu}{\sigma}\right)^2}$$

where σ is the variance (0.8 m), x-μ is depth subtracted from a reference depth, and R_0 is the maximum rate of 0.03 $\mu M\ d^{-1}$. The values chosen for σ and R_0 reproduce the measured sulfate profile and yield volume specific and depth-integrated rates similar to those directly measured in the water column. Minor discrepancies between the depth distributions of the modeled and measured sulfate reduction rates are most likely attributable to seiching, given that sulfate reduction rates and the sulfate profiles were measured at different times and that seiching has an amplitude of 4-10 meters and a period of several hours (*33*). Additional differences can arise from vertical variability in K_z (*33*), which we cannot account for in the current model. Gradients in sulfate concentration were computed by integrating the sulfate reduction rates, and concentrations were then computed through integration of the gradients.

Specific rates of $^{34}SO_4^{2-}$ and $^{32}SO_4^{2-}$ reduction and concentrations of $^{34}SO_4^{2-}$ and $^{32}SO_4^{2-}$ are related by a fractionation factor (α):

$$\alpha = \frac{R_{32SR}[^{34}SO_4^{2-}]}{R_{34SR}[^{32}SO_4^{2-}]}$$

At fractionations of between 20 and 70 ‰, the rate of $^{32}SO_4^{2-}$ reduction (R_{32SR}) ≈ $0.96R_{SR}$ to within one percent, so R_{32SR} was calculated as $0.96R_{SR}$. For our calculations, an initial approximation of R_{34SR} was thus taken as $0.04R_{SR}$. The differential equations required to determine steady-state values of [$^{34}SO_4^{2-}$] and R_{34SR}, were solved numerically. The model was highly sensitive to the initial R_{34SR}, and model convergence was only possible within a narrow range of initial R_{34SR} values. The values for [$^{34}SO_4^{2-}$] and R_{34SR} were obtained iteratively until the model converged on an α within ± <0.0001 of the specified value. For example, if the specified α were 1.020, convergence was deemed acceptable at a modeled α of between 1.0199 and 1.0201. In other words, modeled fractionations were accurate to within ±0.1 ‰ $\delta^{34}S$.

The model was run with α values of 1.020, 1.035 1.045, and 1.070. In addition, variable fractionations were investigated whereby α was set at 1.070 in the upper reaches of the chemocline, and a linear decrease in α was imposed at concentrations of 8, 6, and 4 μM sulfate. The fit of the modeled $\delta^{34}S$ sulfate values to the measured $\delta^{34}S$ sulfate profiles was assessed visually, and of the fractionations tested, a variable fractionation with initial α of 1.070 decreasing linearly below 6 μM sulfate appeared to fit the data best. Lower values for α did not improve the fit, and a better fit would likely require variable K_z and possibly a non-normal distribution in sulfate reduction rates. These factors can be explored in future modeling efforts. Overall, our modeling shows that fractionations higher than 20 ‰ and possibly as high as 70 ‰ are needed to reproduce the measured S-isotope compositions.

The $\delta^{34}S$ of sulfide produced was calculated by subtracting the instantaneous fractionation ((α -1)*1000) at a given depth from the $\delta^{34}S$ of sulfate at the same depth. The $\delta^{34}S$ values, averaged over the water column, for the sulfide exported to the underlying sediments were calculated by integrating $\delta^{34}S*R_{SR}$ over depth. An implicit assumption in this model is that the sulfide produced through microbial sulfate reduction is quantitatively scavenged by reaction with Fe and precipitated as FeS and FeS_2 without recycling through oxidation. There is some evidence for oxidative sulfur cycling in the upper reaches of Lake Matano's chemocline, but as discussed below, this is unlikely to have a significant effect on the $\delta^{34}S$ of exported sulfide.

Sulfide oxidation

Sulfide oxidation and sulfur compound disproportionation reactions can contribute to the fractionations generated during sulfur cycling, and the influence of these processes can be revealed through the specific behavior of ^{33}S compared to ^{34}S (*34, 35*). Such a comparison from sulfate and sulfides in the Lake Matano chemocline produce no evidence for these alternative fractionation pathways (Table S1), implying that fractionations are exclusively due to microbial sulfate reduction. Furthermore, biological sulfur oxidation carries little fractionation (*36, 37*), and appreciable oxidation of

isotopically light sulfide all the way to sulfate would be directly recorded as a negative excursion in the $\delta^{34}S$ of sulfate. The $\delta^{34}S$ of sulfate at the upper margin of the chemocline, where sulfide oxidation would be most intense, is identical to the overlying water, while the $\delta^{34}S$ of sulfate becomes progressively heavier with depth, demonstrating a lack of isotopic effects from sulfide oxidation. If sulfide oxidation to sulfate were to operate cryptically, then the gradient in sulfate $\delta^{34}S$ values would be smaller than without sulfide oxidation, and sulfide oxidation would therefore cause us to underestimate the magnitude of fractionation from sulfate reduction based on sulfate profiles. Likewise, the sulfide exported would be isotopically lighter when oxidation operates, causing an overestimation of fractionation based on comparisons between $\delta^{34}S$ values of sulfide and sulfate.

Archean ocean 1-dimensional reaction-transport models

We constructed a model to explore how sulfate levels in the Archean oceans would influence the fractionation of sulfur isotopes in the ocean water column, and made predictions about how this fractionation would be recorded in the distribution of S-isotopes in marine sedimentary sulfides (pyrite). Like our model for Lake Matano, the model for the Archean ocean water column predicts sulfate distributions under steady-state conditions by describing changes in sulfate with depth as a function of vertical transport and bacterial reduction of sulfate to sulfide as:

$$K_U \frac{\partial^2[SO_4^{2-}]}{\partial x^2} - R_{SR} = 0$$

where K_U is the vertical mixing coefficient (1.728 m^2d^{-1}, (*38*)), x is the depth in the water column, and R_{SR} is the sulfate reduction rate. Sulfate reduction rates were calculated with a Michaelis-Menten description of sulfate reduction kinetics:

$$R_{SR} = \frac{V_{\max}[SO_4^{2-}]}{K_m + [SO_4^{2-}]}$$

where K_m is the half-saturation constant, which was taken as 5 μM for low sulfate environments (*39, 5*). V_{max} is the maximum sulfate reduction rate when sulfate supply is unlimited. When sulfate supply is unlimited, sulfate reduction rates are limited by the availability of organic matter. In the modern ocean, oxygen respiration rates are limited by the availability of organic matter, and we thus take modern open ocean respiration rates (*40*) as a starting point for the estimation of V_{max} (Table S2). Anaerobic respiration rates often appear to be slower than aerobic respiration and we have therefore decreased V_{max} correspondingly (*41*). Finally, primary production in the Archean oceans was likely lower than today, with model-based estimates suggesting a factor of 10 lower (*42*). The volume specific rates of sulfate reduction rendered by our model at low μM sulfate concentrations are well below those measured in Lake Matano's water column, illustrating that such rates are within the physiological capacity of modern sulfate reducing bacteria. They are also much lower than rates of anaerobic nitrate respiration

observed at comparable depths in modern oxygen minimum zones, indicating that marine systems today could support our modeled sulfate reduction rates.

Sulfate gradients, concentrations, as well as the $\delta^{34}S$ of sulfate and sulfide were computed as described above for Lake Matano. We conservatively imposed a fractionation factor of 30 ‰, which is typical for sulfate reducing bacteria (*3)* and also in line with micro-scale $\delta^{34}S$ values from Archean pyrites, and decreased this fractionation linearly below 6 μM, in line with our observations from Lake Matano. We note that higher imposed fractionations would lead to lower estimates for seawater sulfate concentrations. Likewise, if high fractionations persisted below 6 μM, this would also lead to lower estimates for seawater sulfate concentrations. The effect of surface seawater sulfate concentrations on depth profiles of the $\delta^{34}S$ of sulfate and sulfide, as well as the integrated $\delta^{34}S$ of sulfide exported was evaluated by systematically changing the surface seawater sulfate concentration in the model. Integrated pelagic sulfate reduction rates along with the $\delta^{34}S$ of sulfide exported at various surface seawater sulfate concentrations are tabulated below (Table S3).

We have evaluated the sensitivity of our model outputs to the availability of organic matter (Fig. S1). Since a greater availability of organic matter increases sulfate reduction rates, sulfate drawdown is more extensive, and the $\delta^{34}S$ values of exported sulfides are closer to surface seawater sulfate—all other factors being equal. Nevertheless, even at modern day levels of primary production and organic matter availability, fractionations greater than the 15 ‰ observed in the Archean record are expected at sulfate concentrations higher than about 10 μM. Lesser organic matter availability would lead to high fractionations at even lower seawater sulfate concentrations. Our model results then appear to be robust across at least an order of magnitude variability in organic matter availability. We also evaluated the effect of not decreasing fractionation below 6 μM sulfate at organic matter availability, corresponding to 5 times lower primary production than today. The $\delta^{34}S$ of exported sulfide in this case approaches 15 ‰, but remains greater than 15 ‰ to sulfate concentrations below 2.5 μM.

Archean sediment 1-dimensional reaction-transport model

The Archean sediment model was constructed in a similar fashion to the water column model. The reactivity of organic carbon was described by a power law as a function of time: $\log_{10} k = -(0.95) \log_{10} t - (0.81)$. Integrated sediment sulfate reduction rates along with the $\delta^{34}S$ of sulfide produced at various surface seawater sulfate concentrations are tabulated below (Table S4). Relevant sediment parameters are summarized in Table S5 below. Using a constant fractionation factor in the sediment model leads to high sediment sulfide isotope fractionations, even at 1 μM seawater sulfate (Fig. S2). Model runs at various porosities, as well as for porosities that decrease with depth (compaction), reveal a lack (<1.5‰) of sensitivity to porosity, given the same sedimentation flux of organic carbon. These results are consistent with the findings of earlier models of sulfur isotope fractionations. Model runs at various organic matter concentrations and sedimentation velocities also reveal a lack of sensitivity to these parameters.

Biogeochemical implications for low seawater sulfate

Global marine productivity in the Archean has been estimated at up to 5×10^{14} mol C yr^{-1} (*42*), and combining this with an ocean surface area of 3.61×10^{14} m^2 yields

primary production of 1.39 mol C m^{-2} yr^{-1}. Estimated fractions of organic carbon degradation through pelagic sulfate reduction are presented in Table S2. Sulfur is also required by organisms as a nutrient for protein synthesis, and typical modern marine organic matter has a C:S of 48:1 (*31*). In the absence of other sulfur sources, organisms would meet their nutrient S quotas through assimilatory sulfate reduction, which at primary production rates of 1.39 mol C m^{-2} yr^{-1} would occur at a rate of 0.013 mol S m^{-2} yr^{-1}, (35.6×10^{-5} mol S m^{-2} d^{-1}). At surface seawater sulfate concentrations of between 1 and 5 μM, assimilatory sulfate reduction would account for between 82 and 65 %, respectively, of total sulfate reduction. Under the high Fe concentrations predicted for the Archean ocean, the low solubility of FeS would limit sulfide concentrations to sub-μM concentrations (*43*), implying sulfate was the most available pool of sulfur. Elemental S may also have been present, but its concentration and availability are unknown at this time. Elemental sulfur is poorly soluble in water (*44*), so its concentration was likely in the sub-μM range.

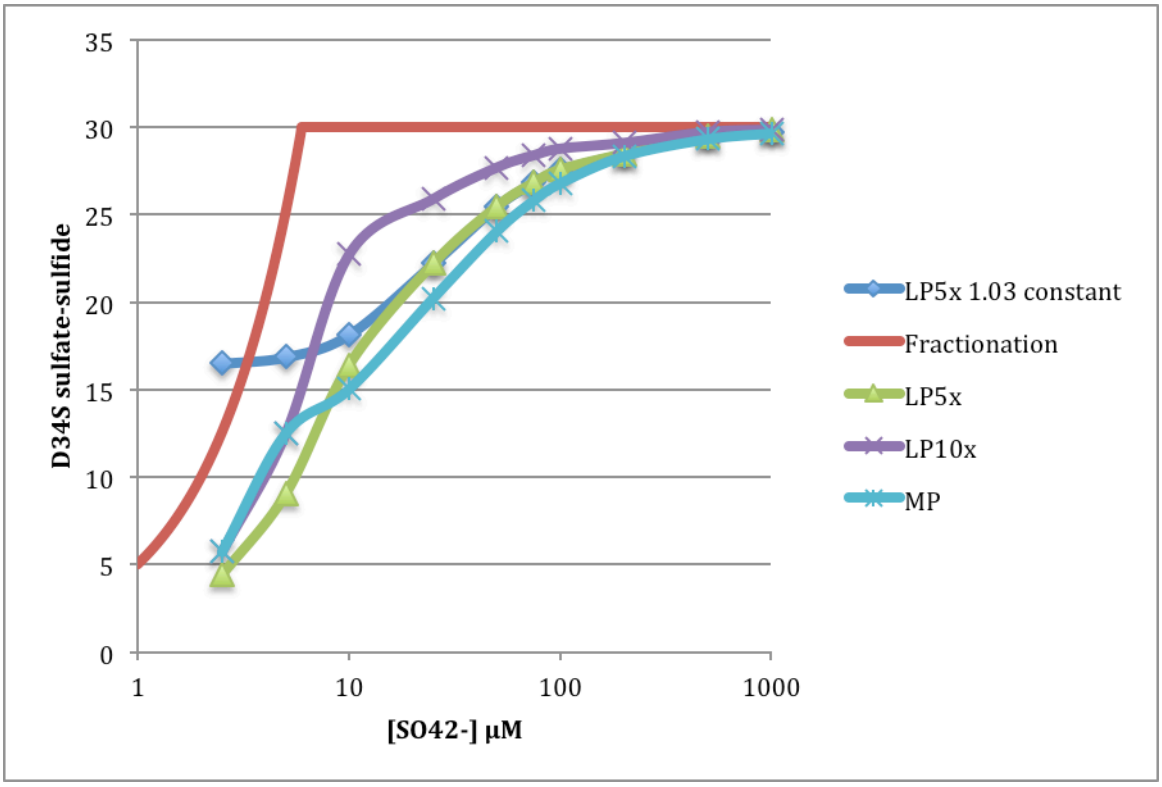

Fig. S1.

Sensitivity of model outputs to organic matter availability. MP corresponds to modern levels of productivity, LP5x and LP10x correspond to 5 and 10 times lower production than today. The red line shows the imposed fractionation of 30 ‰, which is decreased linearly below sulfate concentrations of 6 µM. LP5x 1.03 constant illustrates the effect of not decreasing fractionation below 6 µM at 5x lower organic matter availability than today.

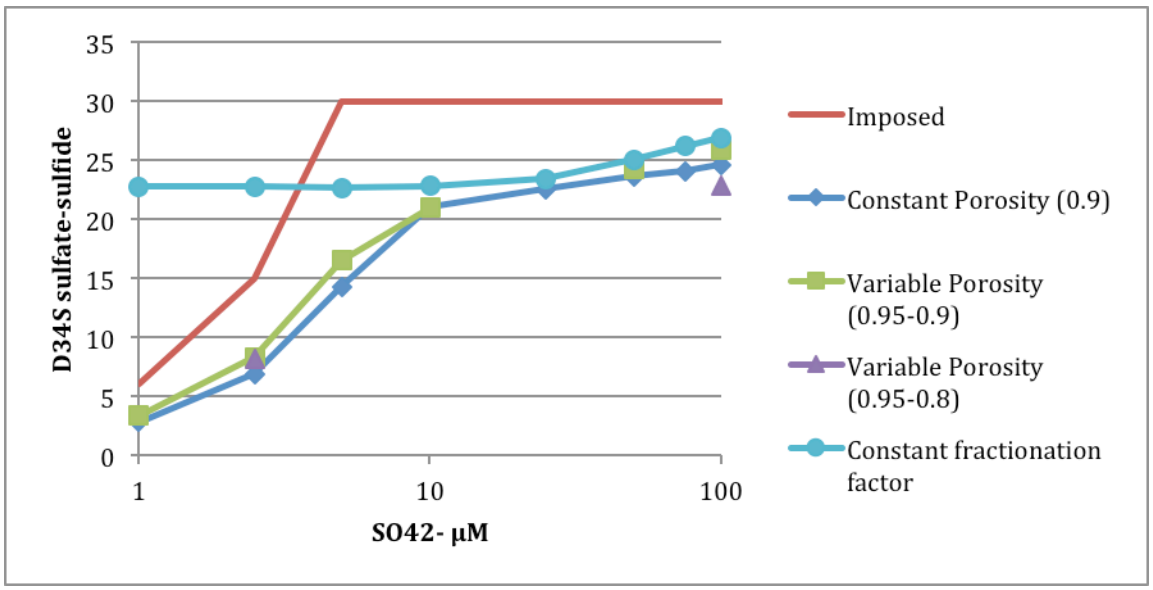

Fig. S2

Sensitivity of sediment model outputs to porosity and variability in the fractionation factor. Model runs include a constant porosity of 0.9 (blue line), variable porosity from 0.95 at the sediment-water interface to 0.9 at 20cm below the sediment-water interface (green line), and variable porosity from 0.95 at the sediment-water interface to 0.8 at 20cm below the sediment-water interface (purple triangles). The red line shows the imposed fractionation of 30 ‰, which is decreased linearly below sulfate concentrations of 6 µM. The cyan line illustrates the effect of not decreasing fractionation below 6 µM sulfate (i.e. a constant α of 1.03).

Table S1.
Sulfur isotope values determined by IR-MS

Depth (m)	Year	Sulfate µM	Technique	Species	$\delta^{34}S$	$\Delta^{33}S$
5	2009	29	SF_6	SO_4^{2-}	10.34	0.012
20	2009	29	SF_6	SO_4^{2-}	9.45	0.007
20	2009	29	SF_6	SO_4^{2-}	9.44	□0.008
20	2009	29	SF_6	SO_4^{2-}	10.1	0.011
125	2009	17	SO_2	AVS	-1.20	
125	2009	17	SF_6	CRS	-13.2	0.009
0	2010	29	SF_6	SO_4^{2-}	10.1	-0.002
0	2010	29	SF_6	SO_4^{2-}	10.7	-0.004
82.5	2010	25	SF_6	SO_4^{2-}	9.8	0.020
130	2010	0	SF_6	AVS	5.4	0.024
130	2010	0	SF_6	CRS	0.1	0.031

Table S2.

Values used to obtain estimates of sulfate reduction V_{max}.

Depth	**Oxygen Respiration mmol m-^{3} yr^{-1}**	**Oxygen Respiration mmol m-^{3} yr^{-1}**	**Sulfate reduction mmol m-^{3} yr^{-1}**	**Sulfate reduction mmol m-^{3} yr^{-1}**
	From(*44*)	Scaled for anoxia(*45*)	Modern OM	10x less
100	21.6	17.28	8.64	0.864
150	10.1	8.08	4.04	0.404
200	5.9	4.72	2.36	0.236
250	3.9	3.12	1.56	0.156

Table S3.

Water column model results including integrated sulfate reduction rates (SRR), and integrated $\delta^{34}S$.

Surface seawater sulfate (µM)	**1**	**2.5**	**5**	**10**	**25**	**50**	**75**	**100**	**200**	**500**	**1000**
SRR mol S m^{-2} d^{-1} ($x10^{-6}$)	7.9	18	30	44	60	67	70	71	73	74	74
$\delta^{34}S$ (‰)	2.2	5.7	12.5	22.7	25.9	27.7	28.4	28.8	29.1	29.7	29.9
% OM degradation	1	2.3	3.9	5.9	8	8.8	9.2	9.3	9.5	9.7	9.8

Table S4
Sediment model results including integrated sulfate reduction rates (SRR), and integrated $\delta^{34}S$.

Surface seawater sulfate (µM)	**1**	**2.5**	**5**	**10**	**25**	**50**	**75**	**100**	**200**	**500**	**1000**
SRR mol S m^{-2} d^{-1} ($x10^{-6}$)	27	61	97	140	198	236	256	268	321	420	338
$\delta^{34}S$ (‰)	2.8	6.9	14.2	21.1	22.6	23.6	24.0	24.6	25.6	27.2	28.0
% OM degradation	6	13	21	31	43	52	56	59	64	70	74

Table S5
Sediment model parameter values

Parameter	**Value**
Sedimentation rate	0.05 g cm^{-2} y^{-1}
Organic carbon flux	228 μmol m^{-2} d^{-1}
Sediment porosity	0.9
K_{mSO42-}	5 μM
Imposed fractionation (at sulfate > 6μM)	30 ‰

Additional Data table S1 (separate file)
Compilation of Archean sediment sulfur isotope data.

References and Notes

1. S. T. Petsch, R. A. Berner, Coupling the geochemical cycles of C, P, Fe, and S; the effect on atmospheric O_2 and the isotopic records of carbon and sulfur. *Am. J. Sci.* **298**, 246–262 (1998). doi:10.2475/ajs.298.3.246

2. B. B. Jørgensen, Mineralization of organic matter in the sea bed—the role of sulphate reduction. *Nature* **296**, 643–645 (1982). doi:10.1038/296643a0

3. D. E. Canfield, Isotope fractionation by natural populations of sulfate-reducing bacteria. *Geochim. Cosmochim. Acta* **65**, 1117–1124 (2001). doi:10.1016/S0016-7037(00)00584-6

4. R. A. Berner, S. T. Petsch, The sulfur cycle and atmospheric oxygen. *Science* **282**, 1426–1427 (1998). doi:10.1126/science.282.5393.1426

5. K. S. Habicht, M. Gade, B. Thamdrup, P. Berg, D. E. Canfield, Calibration of sulfate levels in the Archean ocean. *Science* **298**, 2372–2374 (2002). Medline doi:10.1126/science.1078265

6. Q. J. Guo, H. Strauss, A. J. Kaufman, S. Schroder, J. Gutzmer, B. Wing, M. A. Baker, A. Bekker, Q. Jin, S.-T. Kim, J. Farquhar, Reconstructing Earth's surface oxidation across the Archean-Proterozoic transition. *Geology* **37**, 399–402 (2009). doi:10.1130/G25423A.1

7. I. Halevy, D. T. Johnston, D. P. Schrag, Explaining the structure of the Archean mass-independent sulfur isotope record. *Science* **329**, 204–207 (2010). Medline doi:10.1126/science.1190298

8. J. W. Jamieson, B. A. Wing, J. Farquhar, M. D. Hannington, *Nat. Geosci.* **6**, 61 (2013).

9. I. Halevy, Production, preservation, and biological processing of mass-independent sulfur isotope fractionation in the Archean surface environment. *Proc. Natl. Acad. Sci. U.S.A.* **110**, 17644–17649 (2013). Medline doi:10.1073/pnas.1213148110

10. J. Farquhar, J. Cliff, A. L. Zerkle, A. Kamyshny, S. W. Poulton, M. Claire, D. Adams, B. Harms, Pathways for Neoarchean pyrite formation constrained by mass-independent sulfur isotopes. *Proc. Natl. Acad. Sci. U.S.A.* **110**, 17638–17643 (2013). Medline doi:10.1073/pnas.1218851110

11. W. W. Fischer, D. A. Fike, J. E. Johnson, T. D. Raub, Y. Guan, J. L. Kirschvink, J. M. Eiler, SQUID-SIMS is a useful approach to uncover primary signals in the Archean sulfur cycle. *Proc. Natl. Acad. Sci. U.S.A.* **111**, 5468–5473 (2014). Medline doi:10.1073/pnas.1322577111

12. B. S. Kamber, M. J. Whitehouse, Micro-scale sulphur isotope evidence for sulphur cycling in the late Archean shallow ocean. *Geobiology* **5**, 5–17 (2007).

13. D. E. Canfield, J. Farquhar, A. L. Zerkle, High isotope fractionations during sulfate reduction in a low-sulfate euxinic ocean analog. *Geology* **38**, 415–418 (2010). doi:10.1130/G30723.1

14. M. L. Gomes, M. T. Hurtgen, Sulfur isotope systematics of a euxinic, low-sulfate lake: Evaluating the importance of the reservoir effect in modern and ancient oceans. *Geology* **41**, 663–666 (2013). doi:10.1130/G34187.1

15. M. Nakagawa, Y. Ueno, S. Hattori, M. Umemura, A. Yagi, K. Takai, K. Koba, Y. Sasaki, A. Makabe, N. Yoshida, Seasonal change in microbial sulfur cycling in monomictic Lake Fukami-ike, Japan. *Limnol. Oceanogr*. **57**, 974–988 (2012). doi:10.4319/lo.2012.57.4.0974

16. M. S. Sim, S. Ono, K. Donovan, S. P. Templer, T. Bosak, Effect of electron donors on the fractionation of sulfur isotopes by a marine *Desulfovibrio* sp. *Geochim. Cosmochim. Acta* **75**, 4244–4259 (2011). doi:10.1016/j.gca.2011.05.021

17. W. D. Leavitt, I. Halevy, A. S. Bradley, D. T. Johnston, Influence of sulfate reduction rates on the Phanerozoic sulfur isotope record. *Proc. Natl. Acad. Sci. U.S.A.* **110**, 11244–11249 (2013). Medline doi:10.1073/pnas.1218874110

18. S. A. Crowe, C. Jones, S. Katsev, C. Magen, A. H. O'Neill, A. Sturm, D. E. Canfield, G. D. Haffner, A. Mucci, B. Sundby, D. A. Fowle, Photoferrotrophs thrive in an Archean ocean analogue. *Proc. Natl. Acad. Sci. U.S.A.* **105**, 15938–15943 (2008). Medline doi:10.1073/pnas.0805313105

19. Materials and methods are available as supplementary materials on *Science* Online.

20. G. Paris, A. L. Sessions, A. V. Subhas, J. F. Adkins, MC-ICP-MS measurement of $\delta^{34}S$ and $\Delta^{33}S$ in small amounts of dissolved sulfate. *Chem. Geol.* **345**, 50–61 (2013). doi:10.1016/j.chemgeo.2013.02.022

21. M. B. Goldhaber, I. R. Kaplan, Mechanisms of sulfur incorporation and isotope fractionation during early diagenesis in sediments of the gulf of California. *Mar. Chem.* **9**, 95–143 (1980). doi:10.1016/0304-4203(80)90063-8

22. B. B. Jorgensen, A theoretical model of the stable sulfur isotope distribution in marine sediments. *Geochim. Cosmochim. Acta* **43**, 363–374 (1979). doi:10.1016/0016-7037(79)90201-1

23. S. Ono, J. L. Eigenbrode, A. A. Pavlov, P. Kharecha, D. Rumble III, J. F. Kasting, K. H. Freeman, New insights into Archean sulfur cycle from mass-independent sulfur isotope records from the Hamersley Basin, Australia. *Earth Planet. Sci. Lett.* **213**, 15–30 (2003). doi:10.1016/S0012-821X(03)00295-4

24. S. W. Poulton, D. E. Canfield, Ferruginous conditions: A dominant feature of the ocean through Earth's history. *Elements* **7**, 107–112 (2011). doi:10.2113/gselements.7.2.107

25. D. E. Canfield, F. J. Stewart, B. Thamdrup, L. De Brabandere, T. Dalsgaard, E. F. Delong, N. P. Revsbech, O. Ulloa, A cryptic sulfur cycle in oxygen-minimum-zone waters off the Chilean coast. *Science* **330**, 1375–1378 (2010). Medline doi:10.1126/science.1196889

26. E. M. Cameron, K. Hattori, Archean sulphur cycle: evidence from sulphate minerals and isotopically fractionated sulphides in Superior Province, Canada. *Chem. Geol.* **65**, 341–358 (1987).

27. D. E. Canfield, J. Farquhar, Animal evolution, bioturbation, and the sulfate concentration of the oceans. *Proc. Natl. Acad. Sci. U.S.A.* **106**, 8123–8127 (2009). Medline doi:10.1073/pnas.0902037106

28. I. B. Lambert, T. H. Donnelly, J. S. R. Dunlop, D. I. Groves, Stable isotopic compositions of early Archaean sulphate deposits of probable evaporitic and volcanogenic origins. *Nature* **276**, 808–811 (1978). doi:10.1038/276808a0

29. D. L. Roerdink, P. R. D. Mason, J. Farquhar, T. Reimer, Multiple sulfur isotopes in Paleoarchean barites identify an important role for microbial sulfate reduction in the early marine environment. *Earth Planet. Sci. Lett.* **331–332**, 177–186 (2012). doi:10.1016/j.epsl.2012.03.020

30. E. E. Stüeken, D. C. Catling, R. Buick, Contributions to late Archaean sulphur cycling by life on land. *Nat. Geosci.* **5**, 722–725 (2012). doi:10.1038/ngeo1585

31. C. T. A. Chen, C. M. Lin, B. T. Huang, L. F. Chang, Stoichiometry of carbon, hydrogen, nitrogen, sulfur and oxygen in the particulate matter of the western North Pacific marginal seas. *Mar. Chem.* **54**, 179–190 (1996). doi:10.1016/0304-4203(96)00021-7

32. S. A. Crowe, J. A. Maresca, C. Jones, A. Sturm, C. Henny, D. A. Fowle, R. P. Cox, E. F. Delong, D. E. Canfield, Deep-water anoxygenic photosythesis in a ferruginous chemocline. *Geobiology* **12**, 322–339 (2014). Medline doi:10.1111/gbi.12089

33. S. Katsev, S. A. Crowe, A. Mucci, B. Sundby, S. Nomosatryo, G. D. Haffner, D. A. Fowle, Mixing and its effects on biogeochemistry in the persistently stratified, deep, tropical Lake Matano, Indonesia. *Limnol. Oceanogr.* **55**, 763–776 (2010). doi:10.4319/lo.2009.55.2.0763

34. J. Farquhar, D. T. Johnston, B. A. Wing, K. S. Habicht, D. E. Canfield, S. Airieau, M. H. Thiemens, Multiple sulphur isotopic interpretations of biosynthetic pathways: Implications for biological signatures in the sulphur isotope record. *Geobiology* **1**, 27–36 (2003). doi:10.1046/j.1472-4669.2003.00007.x

35. A. L. Zerkle, A. Kamyshny Jr., L. R. Kump, J. Farquhar, H. Oduro, M. A. Arthur, Sulfur cycling in a stratified euxinic lake with moderately high sulfate: Constraints from quadruple S isotopes. *Geochim. Cosmochim. Acta* **74**, 4953–4970 (2010). doi:10.1016/j.gca.2010.06.015

36. A. L. Zerkle, J. Farquhar, D. T. Johnston, R. P. Cox, D. E. Canfield, Fractionation of multiple sulfur isotopes during phototrophic oxidation of sulfide and elemental sulfur by a green sulfur bacterium. *Geochim. Cosmochim. Acta* **73**, 291–306 (2009). doi:10.1016/j.gca.2008.10.027

37. B. Fry, J. Cox, H. Gest, J. M. Hayes, Discrimination between ^{34}S and ^{32}S during bacterial metabolism of inorganic sulfur compounds. *J. Bacteriol.* **165**, 328–330 (1986). Medline

38. D. E. Canfield, Models of oxic respiration, denitrification and sulfate reduction in zones of coastal upwelling. *Geochim. Cosmochim. Acta* **70**, 5753–5765 (2006). doi:10.1016/j.gca.2006.07.023

39. K. Ingvorsen, B. B. Jørgensen, Kinetics of sulfate uptake by freshwater and marine species of *Desulfovibrio*. *Arch. Microbiol.* **139**, 61–66 (1984). doi:10.1007/BF00692713

40. J. H. Martin, G. A. Knauer, D. M. Karl, W. W. Broenkow, VERTEX: Carbon cycling in the northeast Pacific. *Deep-Sea Res.* **34**, 267–285 (1987). doi:10.1016/0198-0149(87)90086-0

41. A. H. Devol, H. E. Hartnett, Role of the oxygen-deficient zone in transfer of organic carbon to the deep ocean. *Limnol. Oceanogr.* **46**, 1684–1690 (2001). doi:10.4319/lo.2001.46.7.1684

42. D. E. Canfield, M. T. Rosing, C. Bjerrum, Early anaerobic metabolisms. *Philos T R Soc B* **361**, 1819–1836 (2006). doi:10.1098/rstb.2006.1906

43. M. A. Saito, D. M. Sigman, F. M. M. Morel, The bioinorganic chemistry of the ancient ocean: The co-evolution of cyanobacterial metal requirements and biogeochemical cycles at the Archean–Proterozoic boundary? *Inorg. Chim. Acta* **356**, 308–318 (2003). doi:10.1016/S0020-1693(03)00442-0

44. J. Boulègue, Solubility of elemental sulfur in water at 298 K. *Phosphorous Sulfur Relat. Elem.* **5**, 127–128 (1978). doi:10.1080/03086647808069875

45. J. Farquhar, H. Bao, M. Thiemens, Atmospheric influence of Earth's earliest sulfur cycle. *Science* **289**, 756–758 (2000). Medline doi:10.1126/science.289.5480.756

46. J. Farquhar, M. Peters, D. T. Johnston, H. Strauss, A. Masterson, U. Wiechert, A. J. Kaufman, Isotopic evidence for Mesoarchaean anoxia and changing atmospheric sulphur chemistry. *Nature* **449**, 706–709 (2007). Medline doi:10.1038/nature06202

47. A. J. Kaufman, D. T. Johnston, J. Farquhar, A. L. Masterson, T. W. Lyons, S. Bates, A. D. Anbar, G. L. Arnold, J. Garvin, R. Buick, Late Archean biospheric oxygenation and atmospheric evolution. *Science* **317**, 1900–1903 (2007). Medline doi:10.1126/science.1138700

48. P. Philippot, M. Van Zuilen, K. Lepot, C. Thomazo, J. Farquhar, M. J. Van Kranendonk, Early Archaean microorganisms preferred elemental sulfur, not sulfate. *Science* **317**, 1534–1537 (2007). Medline doi:10.1126/science.1145861

49. A. L. Zerkle, M. Claire, S. D. Domagal-Goldman, J. Farquhar, S. W. Poulton, A bistable organic-rich atmosphere on the Neoarchaean Earth. *Nat. Geosci.* **5**, 359–363 (2012). doi:10.1038/ngeo1425

50. K. J. Hou, Y. H. Li, D. F. Wan, Constraints on the Archean atmospheric oxygen and sulfur cycle from mass-independent sulfur records from Anshan-Benxi BIFs, Liaoning Province, China. *Sci. China Ser. D Earth Sci.* **50**, 1471–1478 (2007). doi:10.1007/s11430-007-0106-9

51. S. D. Domagal-Goldman, J. F. Kasting, D. T. Johnston, J. Farquhar, Organic haze, glaciations and multiple sulfur isotopes in the Mid-Archean Era. *Earth Planet. Sci. Lett.* **269**, 29–40 (2008). doi:10.1016/j.epsl.2008.01.040

52. Y. Ueno, S. Ono, D. Rumble, S. Maruyama, Quadruple sulfur isotope analysis of ca. 3.5 Ga Dresser Formation: New evidence for microbial sulfate reduction in the early Archean. *Geochim. Cosmochim. Acta* **72**, 5675–5691 (2008). doi:10.1016/j.gca.2008.08.026

53. S. H. Ono, N. J. Beukes, D. Rumble, Origin of two distinct multiple-sulfur isotope compositions of pyrite in the 2.5 Ga Klein Naute Formation, Griqualand West Basin, South Africa. *Precambrian Res.* **169**, 48–57 (2009). doi:10.1016/j.precamres.2008.10.012

54. Y. N. Shen, J. Farquhar, A. Masterson, A. J. Kaufman, R. Buick, Evaluating the role of microbial sulfate reduction in the early Archean using quadruple isotope systematics. *Earth Planet. Sci. Lett.* **279**, 383–391 (2009). doi:10.1016/j.epsl.2009.01.018

55. C. Thomazo, M. Ader, J. Farquhar, P. Philippot, Methanotrophs regulated atmospheric sulfur isotope anomalies during the Mesoarchean (Tumbiana Formation, Western Australia). *Earth Planet. Sci. Lett.* **279**, 65–75 (2009). doi:10.1016/j.epsl.2008.12.036

56. B. M. Guy, S. Ono, J. Gutzmer, A. J. Kaufman, Y. Lin, M. L. Fogel, N. J. Beukes, A multiple sulfur and organic carbon isotope record from non-conglomeratic sedimentary rocks of the Mesoarchean Witwatersrand Supergroup, South Africa. *Precambrian Res.* **216–219**, 208–231 (2012). doi:10.1016/j.precamres.2012.06.018

57. S. J. Mojzsis, C. D. Coath, J. P. Greenwood, K. D. McKeegan, T. M. Harrison, Mass-independent isotope effects in Archean (2.5 to 3.8 Ga) sedimentary sulfides determined by ion microprobe analysis. *Geochim. Cosmochim. Acta* **67**, 1635–1658 (2003). doi:10.1016/S0016-7037(03)00059-0

58. A. Bekker, H. D. Holland, P. L. Wang, D. Rumble III, H. J. Stein, J. L. Hannah, L. L. Coetzee, N. J. Beukes, Dating the rise of atmospheric oxygen. *Nature* **427**, 117–120 (2004). Medline doi:10.1038/nature02260

59. M. J. Whitehouse, B. S. Kamber, C. M. Fedo, A. Lepland, Integrated Pb- and S-isotope investigation of sulphide minerals from the early Archaean of southwest Greenland. *Chem. Geol.* **222**, 112–131 (2005). doi:10.1016/j.chemgeo.2005.06.004

60. N. L. Cates, S. J. Mojzsis, Chemical and isotopic evidence for widespread Eoarchean metasedimentary enclaves in southern West Greenland. *Geochim. Cosmochim. Acta* **70**, 4229–4257 (2006). doi:10.1016/j.gca.2006.05.014

61. S. H. Ono, A. J. Kaufman, J. Farquhar, D. Y. Sumner, N. J. Beukes, Lithofacies control on multiple-sulfur isotope records and Neoarchean sulfur cycles. *Precambrian Res.* **169**, 58–67 (2009). doi:10.1016/j.precamres.2008.10.013

62. G. X. Hu, D. Rumble, P. L. Wang, An ultraviolet laser microprobe for the in situ analysis of multisulfur isotopes and its use in measuring Archean sulfur isotope mass-independent anomalies. *Geochim. Cosmochim. Acta* **67**, 3101–3118 (2003). doi:10.1016/S0016-7037(02)00929-8

63. H. Ohmoto, Y. Watanabe, H. Ikemi, S. R. Poulson, B. E. Taylor, Sulphur isotope evidence for an oxic Archaean atmosphere. *Nature* **442**, 908–911 (2006). Medline doi:10.1038/nature05044

64. M. A. Partridge, S. D. Golding, K. A. Baublys, E. Young, Pyrite paragenesis and multiple sulfur isotope distribution in late Archean and early Paleoproterozoic Hamersley Basin sediments. *Earth Planet. Sci. Lett.* **272**, 41–49 (2008). doi:10.1016/j.epsl.2008.03.051

65. B. Kendall, C. T. Reinhard, T. W. Lyons, A. J. Kaufman, S. W. Poulton, A. D. Anbar, Pervasive oxygenation along late Archaean ocean margins. *Nat. Geosci.* **3**, 647–652 (2010). doi:10.1038/ngeo942

66. S. D. Golding, in *Earliest Life on Earth: Habitats, Environments and Methods of Detection*, S. D. Golding, M. Glikson, Eds. (Springer, Berlin, 2011), pp. 15–49.

67. D. Papineau, S. J. Mojzsis, Mass-independent fractionation of sulfur isotopes in sulfides from the pre-3770 Ma Isua Supracrustal Belt, West Greenland. *Geobiology* **4**, 227–238 (2006). doi:10.1111/j.1472-4669.2006.00083.x

68. P. Philippot, M. van Zuilen, C. Rollion-Bard, Variations in atmospheric sulphur chemistry on early Earth linked to volcanic activity. *Nat. Geosci.* **5**, 668–674 (2012). doi:10.1038/ngeo1534